Cellular and Molecular Neurobiology (2019) 39:123–135
https://doi.org/10.1007/s10571-018-0638-x

ORIGINAL RESEARCH

APC-Cdh1 Regulates Neuronal Apoptosis Through Modulating Glycolysis and Pentose-Phosphate Pathway After Oxygen-Glucose Deprivation and Reperfusion

Zuofan Li[1] · Bo Zhang[1] · Wenlong Yao[1] · Chuanhan Zhang[1] · Li Wan[1] · Yue Zhang[1]

Received: 14 August 2018 / Accepted: 14 November 2018 / Published online: 20 November 2018
© Springer Science+Business Media, LLC, part of Springer Nature 2018

Abstract

Anaphase-promoting complex (APC) with its coactivator Cdh1 is required to maintain the postmitotic state of neurons via degradation of Cyclin B1, which aims to prevent aberrant cell cycle entry that causes neuronal apoptosis. Interestingly, evidence is accumulating that apart from the cell cycle, APC-Cdh1 also involves in neuronal metabolism via modulating the glycolysis promoting enzyme, 6-phosphofructo-2-kinase/fructose-2,6-bisphosphatase-3 (PFKFB3). Here, we showed that under oxygen-glucose deprivation and reperfusion (OGD/R), APC-Cdh1 was decreased in primary cortical neurons. Likewise, the neurons exhibited enhanced glycolysis when oxygen supply was reestablished during reperfusion, which was termed as the "neuronal Warburg effect." In particular, the reperfused neurons showed elevated PFKFB3 expression in addition to a reduction in glucose 6-phosphate dehydrogenase (G6PD). Such changes directed neuronal glucose metabolism from pentose-phosphate pathway (PPP) to aerobic glycolysis compared to the normal neurons, resulting in increased ROS production and apoptosis during reperfusion. Pretreatment of neurons with Cdh1 expressing lentivirus before OGD could reverse this metabolic shift and attenuated ROS-induced apoptosis. However, the metabolism regulation and neuroprotection by Cdh1 under OGD/R condition could be blocked when co-transfecting neurons with Ken box-mut-PFKFB3 (which is APC-Cdh1 insensitive). Based on these data, we suggest that the Warburg effect may contribute to apoptotic mechanisms in neurons under OGD/R insult, and targeting Cdh1 may be a potential therapeutic strategy as both glucose metabolic regulator and apoptosis suppressor of neurons in brain injuries.

Keywords Aerobic glycolysis · Cdh1 · Neuron · Oxygen-glucose deprivation · Pentose-phosphate pathway

Introduction

Oxidative stress and damage are known to be involved in brain injuries such as cerebral ischemia and reperfusion which occurs in stroke and cardiac arrest. Reactive oxygen radicals, as byproducts of oxidative metabolism during reperfusion, are constantly overproduced by prooxidant enzymes, whereas the endogenous detoxification is disturbed resulting from antioxidant consumption and failure to replenish adequately (Chan 2001). The imbalance between ROS production and cellular antioxidative defense in ischemic brain tissue can induce direct cellular damage to protein, lipid, and DNA, which subsequently causes adverse effects on neuronal cell death (Liu et al. 2001). Neurons are highly fragile to ROS damage, due to their week antioxidant reserve (Schapira 2009).

Recent studies have emphasized the relevance of the antioxidant state and glucose metabolism in control of neuronal survival. Cortical neurons have been shown to naturally express very low glycolytic rate when compared to astrocytes, due to the absence of the glycolytic promoting enzyme, 6-phosphofructo-2-kinase/fructose-2,6-bisphosphatase-3 (PFKFB3) in neurons (Bolaños et al. 2010). PFKFB3 contains a KEN box which can be recognized as proteasomal degradation target by E3 ubiquitin ligase,

Electronic supplementary material The online version of this article (https://doi.org/10.1007/s10571-018-0638-x) contains supplementary material, which is available to authorized users.

✉ Yue Zhang
y.zhang0604@hotmail.com

[1] Department of Anesthesiology, Tongji Hospital, Tongji Medical College, Huazhong University of Science and Technology, 1095 Jiefang Avenue, Wuhan 430030, China

anaphase-promoting complex (APC) with its coactivator Cdh1.

In the normal state, the continuous degradation of PFKFB3 by APC-Cdh1 keeps neurons in a very low glycolytic state. Since the glycolysis and pentose-phosphate pathway (PPP) share the common intermediate glucose-6-phosphate (G6P), the lower glycolysis makes the majority of glucose being oxidized through PPP (Herrero-Mendez et al. 2009). PPP functions as the cellular antioxidant pathway which generates NADPH to maintain glutathione (GSH) to scavenge ROS. Recent reports had shown that neurons exhibited variable glucose metabolic characteristics under different bioenergetic crisis: excitotoxic stimulus of glutamate or NMDA yielded neurons having a higher glycolysis and lower PPP (Rodriguez-Rodriguez et al. 2012), whereas neurons pretreated with low dose of peroxynitrite ($ONOO^-$) exhibited higher PPP activity and resulted in transient resistance to further nitrosative stress (Garcia-Nogales et al. 2003; Bolaños et al. 2008; Bolaños and Almeida 2010). Nevertheless, few information is available regarding the neuronal glucose metabolic alterations under stress made by ischemia/reperfusion insult. Our previous studies demonstrated that Cdh1 of neurons exported from nuclear into cytoplasm, indicative of inactivation of APC-Cdh1, during the reperfusion periods after transient global cerebral ischemia (tGCI) in vivo (Zhang et al. 2011). We have also shown that intrahippocampal injection of Cdh1 overexpression lentivirus before tGCI could mitigate oxidative stress and alleviate neuronal death caused by ischemia (Zhang et al. 2018). We thus are encouraged to explore if the change of APC-Cdh1 second to ischemia/reperfusion may contribute to switch of neuronal glucose metabolism and its induction could increase endogenous antioxidant capability through PPP in neurons, thus protecting neurons against ROS damage in an in vitro model of oxygen-glucose deprivation and reperfusion (OGD/R).

Materials and Methods

Animals

Timed-pregnant Sprague–Dawley rats (14–15 days of gestation) purchased from Tongji Medical College Experimental Animal Center were housed at the Tongji Medical College animal facilities. Primary cultured neurons were prepared from E15 rat embryos. All studies were performed in accordance with National Institutes of Health (NIH) Guidelines for the Care and Use of Laboratory Animals, and protocols were approved by the Experimental Animal Care and Use Committee of Tongji Medical College, Huazhong University of Science and Technology (Wuhan, China).

Primary Neuronal Cultures

Primary neuronal cultures were prepared from cerebral cortices of E15 Sprague–Dawley rat embryos using a modification of a previously described procedure (McLaughlin et al. 1998). Briefly, dissected cerebral cortices were minced and dissociated with 0.25 mg/ml trypsin-EDTA for 15 min at 37 °C and then rinsed with Dulbecco's Modified Eagle Medium (DMEM)/Nutrient Mixture F-12 containing of 10% Fetal Bovine Serum (FBS) (Invitrogen, USA). Tissue pieces were triturated by a pipette and then passed through a 40-μm mesh strainer (BD Falcon, USA). Isolated cells were then suspended in DMEM/ F12 containing of 10% FBS and 1% penicillin/streptomycin, plated at a lower density (1×10^5 cells/ cm^2 for immunocytochemistry) in 10 μg/ml poly-D-lysine-coated 12-mm coverslips, and a higher density (5×10^5 cells/ cm^2 for metabolism and Western blot analysis) in coated 6-well plates, and incubated at 37 °C in a 95%/5% mixture of atmospheric air and CO_2. The medium was replaced after 4 h by Neurobasal medium supplemented with B27, L-glutamine, and 1% penicillin/streptomycin (Invitrogen, USA). At DIV (day in vitro) 4, one-half feeding medium was replaced and 2 μM cytosine arabinoside (AraC) was added to prevent non-neuronal proliferation. Experiments were performed in cells at DIV 7. The cultures contained > 95% neurons as tested by immunocytochemical staining with microtubule-associated protein 2 (MAP2).

Oxygen-Glucose Deprivation and Reperfusion (OGD/R)

Oxygen-glucose deprivation and reperfusion model was performed as previously described (Huang et al. 2008). Briefly, neurons were washed twice and incubated in glucose-free DMEM (Invitrogen, USA), and then placed in a hypoxic incubator filled with a gas mixture of 95% N_2 and 5% CO_2 at 37 °C for 1 h. After OGD, cultures were restored with standard medium and returned to a normoxic incubator under 5% CO_2/95% air for additional 12-h reoxygenation/glucose restoration (reperfusion). For each experiment, cells which were not exposed to OGD were used as control.

Cdh1-Expressing Vector Construction and Lentivirus Intervention

Cdh1-expressing lentivirus vector was previously constructed by our laboratory and proven efficient in vitro and in vivo (Qiu et al. 2013; Lv et al. 2015; Hu et al. 2016; Tan et al. 2015; Zhang et al. 2018). Briefly, the CDS (coding sequence, located in bases 245–544) of rat Cdh1 gene (accession number NM_001108074.1) was chemically

synthesized and amplified by PCR. The sequence was subsequently inserted into the cloning pGC-FU-GFP vector under the control of the cytomegalovirus promoter. The positive recombinant pGC-FU-GFP-Cdh1 was verified by PCR analysis and DNA sequencing. The negative control vector (pGC-FU-GFP-NC) was inserted by a nonsense sequence to control any effects caused by transfection mechanisms. Then pGC-FU-GFP-Cdh1/pGC-FU-GFP-NC and plasmids mix were co-transfected into 293T cells. The lentivirus supernatant was collected at 72 h after transfection, filtered through a 0.45 μm membrane, and then concentrated by ultracentrifugation and titered to 2×10^9 transducing units/ml (TU/ml). As the lentivirus can express green fluorescent protein (GFP), the optimal multiplicity of infection (MOI) and infection duration was determined according to the expression of GFP under fluorescence microscopy. DIV 7 neurons were infected with pGC-FU-GFP-Cdh1/pGC-FU-GFP-NC for 8 h at an MOI of 2 and then the virus particles were washed away with replacement of new culture medium. At 72 h after lentivirus treatment (DIV 10), cells were subjected to OGD.

PFKFB3 Mutagenesis

The site-directed PFKFB3 mutagenesis was obtained as described previously (Herrero-Mendez et al. 2009; Rodriguez-Rodriguez et al. 2012). Briefly, the total length of rat PFKFB3 cDNA (accession number BAA 21754) was chemically synthesized and amplified by PCR. The sequence was subsequently inserted into the cloning pGC-FU-GFP vector. Then the pGC-FU-GFP-PFKFB3 recombinant was subjected to site-directed mutagenesis of its KEN box to AAA using the QuikChange XL site-directed mutagenesis kit (#200517 Stratagene, USA). The functional evaluation of the PFKFB3 mut was presented in Supplementary Fig. 2, which showed that Cdh1 expressing lentivirus promoted the degradation of endogenous increased PFKFB3 following OGD/R, but did not affect its Ken box-mutant form (PFKFB3 mut).

PFKF-1 Plasmid Construction

The full length of human muscle PFK-1 gene sequence (accession number NM_000289) was chemically synthesized and amplified by PCR. The sequence was subsequently sub-cloned in pCDNA3.0 vector. The transfection of this plasmid vector in neurons was performed at DIV 7, followed by exposure to OGD/R.

Western Blot Analysis

Neurons grown on 6-well plates and subjected to treatment described above were lysed with RIPA Lysis Buffer (Thermo Scientific, USA). Protein concentrations were determined with a bicinchoninic acid (BCA) protein assay kit (Thermo Scientific, USA) according to the manufacturer's instructions. Equal amounts of protein samples (total protein extracts, 30 μg) were separated by electrophoresis in 4–15% SDS–polyacrylamide gels (Mini-PROTEAN TGX precast gel, Bio-Rad, USA) and transferred to polyvinylidene fluoride (PVDF) membranes. After blocking, membranes were incubated with primary antibodies against Cdh1 (NBP2-15840, 1:400, Novus Biologicals, USA), SnoN (ab58846, 1:400, Abcam, UK), Skp2 (sc7164, 1:600, Santa Cruz Biotechnology, USA), Pfkfb3 (ab18181, 1:400, Abcam, UK), G6PD (ab993, 1:800, Abcam, UK), Cleaved-Caspase 3 (9664, 1:300, Cell Signaling Technology, USA), GAPDH antibody (sc365062, 1:1000, Santa Cruz Biotechnology, USA) overnight at 4 °C, and the membranes were then incubated with horseradish peroxidase (HRP)-conjugated secondary antibody (1:10000, Cell Signaling Technology, USA) for 1 h at room temperature. The blots were detected by enhanced chemiluminescence (ECL) reagents (Thermo Scientific, USA) and exposed in the ChemiDox XRS station (Bio-Rad). Signals were quantified using Quantity One software 4.62 (Bio-Rad, USA).

Measurement of Glycolysis

The glycolytic flux was measured by tracing the release of ^3H_2O from [5-^{3}H]-glucose as described previously (Vander et al. 2010; TeSlaa and Teitell 2014; Støttrup et al. 2010). Briefly, 1×10^6 neurons were washed with PBS prior to resuspension and incubation in Krebs buffer in vials at 37 °C, 5% CO_2 for 45 min. The buffer was then replaced by 1 ml Krebs buffer containing 10 μCi [5-^{3}H]-glucose (#NET531005MC, Perkin Elmer, USA) and 10 mM unlabeled glucose. Extra oxygen was supplied to those vials for 3 min before sealed. After that, the vials were incubated at 37 °C, 5% CO_2 for 90 min, and the reaction was stopped by 0.2 N HCl. Then, the samples were spun down, and all the supernatants were removed to pass through Poly-Prep chromatography column (#731-1550, Bio-Rad, USA) packed with AG 1-X8 resin (#140-1454, Bio-Rad, USA), which aimed to separate ^3H_2O from [5-^{3}H]-glucose by anion exchange chromatography. After the glucose removal, the ^3H_2O was dissolved into scintillation solution and then quantified by liquid scintillation counter (LS 6500, Beckman, USA). The results of D.P.M were converted to nmol and normalized to sample protein weight.

Measurement of PPP

The PPP flux was measured by tracing the differences of $^{14}CO_2$ production from [1-^{14}C]-glucose (decarboxylated both via the PPP and the tricarboxylic acid cycle) to [6-^{14}C]-glucose (decarboxylated only via the tricarboxylic acid cycle) as described previously (Garcia-Nogales et al. 2003; Larrabee

1990). Briefly, resuspended neurons were transfected to scintillation vials equipped with a central well containing benzethonium hydroxide, with the medium of Krebs buffer containing 1 μCi [1-^{14}C]-glucose or 1 μCi [6-^{14}C]-glucose (#NEC043 × 050UC and #NEC045 × 050UC, Perkin Elmer, USA). The vials were flushed with extra oxygen and then sealed for incubation in water bath with shaking at 100r.p.m. at 37 °C for 45 min. After that, 0.2N HCl was injected into the samples to stop the reaction, and the generated $^{14}CO_2$ was diffused into benzethonium hydroxide, which was then dissolved into scintillation solution and quantified by liquid scintillation counter (LS 6500, Beckman, USA).

Detection of ROS

ROS detection was performed as per the manufacturer's instruction (ab 113851, Abcam, UK). Neurons were incubated with 2′,7′-dichlorofluorescin diacetate (DCFDA, 20 μM, 100 μl/well) for 20 min at 37 °C in the dark. DCFDA, a non-fluorescent compound, can be oxidized by ROS into 2′, 7′-dichlorofluorescin (DCF), a highly fluorescent compound, whose signaling was detected by the Microplate Readers with excitation and emission wavelength at 495 nm and 529 nm, respectively.

In Situ Labeling of Fragmented DNA and Immunocytochemistry

Terminal deoxynucleotidyl transferase (TdT)-mediated dUTP Nick-End labeling (TUNEL) staining was carried out according to the manufacturer's instruction (In situ cell death detection kit, Roche, Germany). Briefly, neurons grown on coverslips and subjected to treatment described above were fixed for 30 min in 4% paraformaldehyde and blocked with 3% H_2O_2 in methanol. After three washed with PBS, the cells were treated with permeabilization solution (0.1% TritonX-100) on ice for 2 min and then incubated with TUNEL reaction buffer containing TdT enzyme and fluorescein-labeled nucleotide mixture for 60 min at 37 °C in humidified chamber. The reaction was terminated by rinse with PBS. In the second step, the cells were incubated with MAP2 antibody (ab11267, 1:200, Abcam, UK) at 4 °C overnight and then incubated with Alexa Fluor 568-conjugated goat anti-mouse IgG antibody (A-11004, 1:400, Invitrogen, USA) for 1 h at room temperature. Coverslips were washed 3 × 5 min with PBS between each step. Coverslips were mounted onto glass slides using mounting medium with DAPI (Vector Laboratories, USA). Images were recorded by fluorescence microscopy and the number of apoptotic neurons was determined by counting the MAP2/TUNEL double-stained cells. The cell number was examined by counting 3 different fields of view on each coverslip.

Statistical Analysis

All data were expressed as mean ± standard deviation (SD) and analyzed by SPSS 19.0. Student's t-test was used as appropriate for comparison between different groups. One-way ANOVA followed by Fisher's LSD post hoc test was used for group comparisons. Statistical significance was defined at $P < 0.05$.

Results

The Effect of 1-h OGD and 12-h Reperfusion on Neuronal Viability and Cdh1 Expression

Triple-labeling with MAP2, TUNEL, and DAPI was used to identify the effect of OGD on neuronal viability. Compared with the control group, 1-h OGD alone caused a significant reduction in viable neurons (99.6 ± 0.06% vs 46.8%±2.65%, $P < 0.05$) (Supplementary Fig. 1), whereas further damage occurred following 12-h reperfusion with neuronal viability decreased to 30.8% (Fig. 1). The expression of Cdh1 in neurons was measured immediately after OGD/R by Western blot. Relative to control, OGD/R led to a significant reduction of Cdh1 (84.15 ± 5.12% vs 58.45 ± 5.60%, $P < 0.05$, the relative expression was normalized to GAPDH). Meanwhile, to test if this reduction would affect Cdh1 mediated-ubiquitinated degradation, we picked 2 of its ubiquitinated substrates, SnoN and Skp2. The ski novel-related gene product SnoN that acts as the transcriptional repressor of TGFβ-Smad2 signaling is a critical substrate of APC-Cdh1 in the control of axonal growth (Stegmüller et al. 2006). Skp2 is an F-box protein of the SKP1-CUL1-F-box (SCF) complex that targets CDK inhibitors for degradation (Bashir et al. 2004). We found that accompanied with Cdh1 reduction, SnoN and Skp2 were significantly increased following OGD/R, compared with control (Fig. 1b). Thus, Cdh1 was decreased with reduced ubiquitination activity after OGD/R.

Cdh1-Expressing Lentivirus Transduction and Identification

The transduction efficiency of Cdh1-expressing lentivirus (pGC-FU-GFP-Cdh1) was assessed by transducing primary cortical neurons and monitoring GFP expression under fluorescence microscopy. DIV 7 neurons were exposed to the lentivirus at MOI of 1, 2, and 4. We found that the percentage of GFP-positive cells reached approximately 68%, 84%, and 90%, respectively (Fig. 2a), indicating the transduction efficiency was increased in an MOI-dependent manner. For the consideration of less toxicity, MOI of 2 was determined to infect primary neurons for the following experiment. Figure 2b demonstrated that neurons infected with MOI of 2 exhibited rare

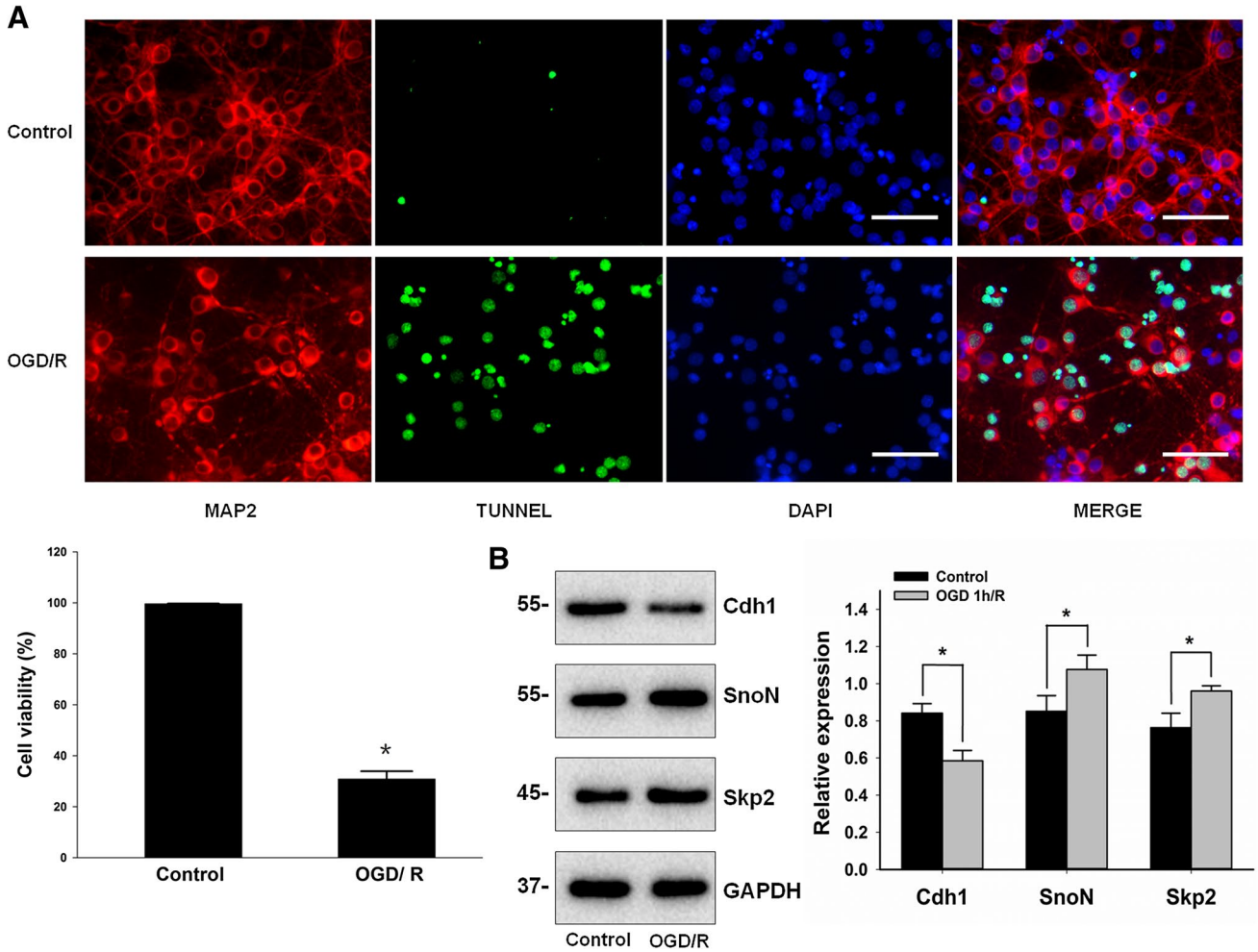

Fig. 1 Effect of 1-h OGD and 12-h reperfusion on neuronal viability and Cdh1 expression. **a** Neurons were exposed to normal condition or OGD/R and then labeled with MAP2 (red), TUNEL (green), and DAPI (blue). The percentage of viable neurons was calculated from the percentage of DAPI stained nuclei that were not co-stained with TUNEL. Three different fields of view on each coverslip were counted and averaged from three independent trials. Bar graph represents percentage of vital neurons with value shown as Mean ± SD, $^*P < 0.05$ vs Control. Scale bars, 50 µm. **b** As shown in Western blot, compared with the normoxia group, the expression of Cdh1 in neurons was significantly decreased after 1-h OGD and 12-h reperfusion, while its ubiquitinated substrates Skp2 and SnoN were increased ($P < 0.05$). The relative expressions of Cdh1, SnoN, and Skp2 were quantified by QUANTITY ONE (Bio-Rad) and then normalized to their internal controls (GAPDH). Data from four independent experiments are shown as mean ± SD. $^*P < 0.05$ vs Control

toxicity, revealed by MAP2, TUNEL, and DAPI triple-staining. To evaluate whether Lenti-Cdh1 infection could result in Cdh1 overexpressing, the neurons cell lysates were tested by Western blot at 72 h after transduction, a fusion protein band (Cdh1-GFP) of approximate 38 kDa was measured, as shown in Fig. 2c. Given that the construction of pGC-FU-Cdh1 was based on CDS of rat Cdh1 gene (NM_001108074.1), but not the full length of the gene, the size of the resultant fusion protein (38 kDa) was less than Cdh1 (55 kDa) by Western blot. Using the Cdh1 lentivirals in our previous study, such a fusion band was found *in vitro and in vivo* as well (Qiu et al. 2013; Lv et al. 2015; Hu et al. 2016; Tan et al. 2015). The fusion band did not appear in cells infected with Lenti-control. Furthermore, we also found that the downstream substrates of APC-Cdh1, Skp2 and SnoN, were significantly decreased after Lenti-Cdh1 infection, compared with the Lenti-control treatment, which indicated that Cdh1 expressed by lentivirus is functional and has E3 ligase degradation activity. In addition, the localization and phosphorylation status of Cdh1/Cdh1-GFP in control and OGD/R condition were also tested. OGD/R induced endogenous Cdh1 transport from nuclei to cytoplasm. However, the fusion protein of Cdh1-GFP localized predominantly to nuclear fraction with a few amount distributed in the cytoplasm in the control group. OGD/ R did not alter the localization of Cdh1-GFP, which remained mainly at the nuclei (Fig. 3a). For the phosphorylation, we observed that the cytoplasmic Cdh1-GFP migration in SDS–PAGE was slowed-shifted than nuclear Cdh1-GFP, suggesting a

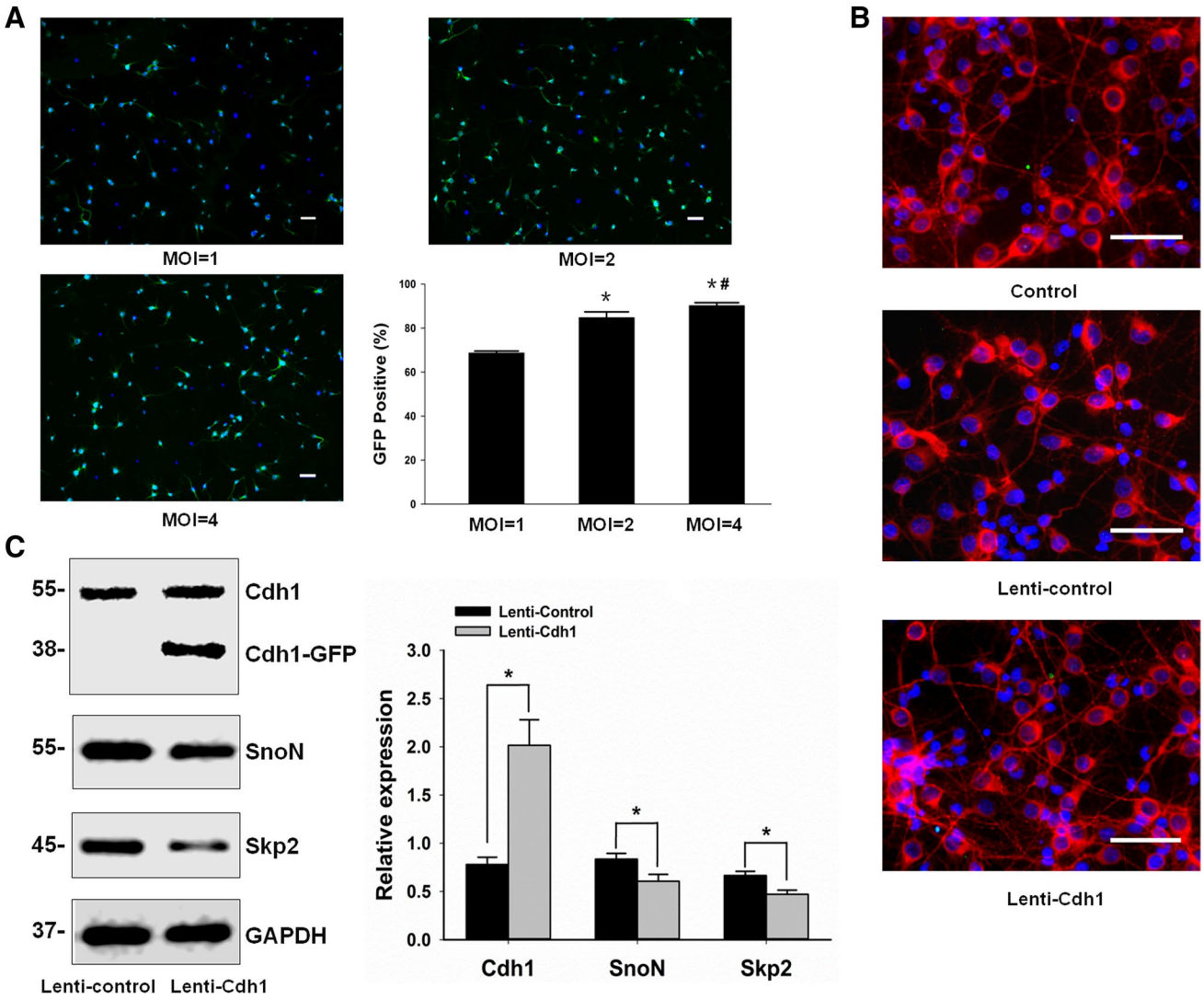

Fig. 2 The identification of Cdh1 expressing lentivirus by Western blot. **a** Neurons were infected with Cdh1 expressing lentivirus at MOI of 1, 2, and 4. 72 h after initial infection, neurons were stained with DAPI, then the infected cells expressing GFP were visualized using a fluorescent microscope, scale bars, 50 µm. Graph of transduction efficacy showed the percentage of GFP- positive neurons compared to total neurons (DAPI positive) after exposure to Lenti-Cdh1 at an MOI ranging from 1 to 4. The transduction efficacy was increased in an MOI-dependent manner. Data from three independent experiments are shown as mean ± SD. $^{*}P<0.05$, $^{\#}P<0.05$ vs MOI 1 and MOI 2. **b** Neurons were treated with Cdh1 expressing or vehicle lentivirus at MOI of 2, which demonstrated rare cytotoxicity, revealed by MAP2 (red), TUNEL (green), and DAPI (blue) triple-staining, scale bars, 50 µm. **c** The fusion protein (Cdh1-GFP) was detected after 72 h of Lenti-Cdh1 infection (at MOI of 2) in neurons in vitro, and the total Cdh1 expression was significantly increased to approximately 2.6 fold of the level found in the vehicle, while its ubiquitinated substrates, SnoN and Skp2, were markedly reduced by Cdh1 expressing lentivirus infection. The relative expressions of Cdh1, SnoN, and Skp2 were quantified by QUANTITY ONE (Bio-Rad) and then normalized to their internal controls (GAPDH). Data from four independent experiments are shown as mean ± SD. $^{*}P<0.05$ vs Lenti-control

post-translational modification on Cdh1-GFP protein in cytoplasm, such as phosphorylation. We then incubated the nuclear and cytoplasmic protein extracts obtained from neurons pretreated with Lenti-Cdh1 in control or OGD/ R group with protein phosphatase. As shown in Fig. 3b, phosphatase treatment converted the cytoplasmic Cdh1-GFP shifted band to the fast-migrating form, while it had no effect on the migration speed of the nuclear band, in both control and OGD/ R group, suggesting that the predominantly nuclei-localized Cdh1-GFP was non-phosphorylated, whereas the sparsely cytoplasm-distributed Cdh1-GFP was phosphorylated.

Cdh1 Deficiency Shifts Neuronal Glucose Metabolism Towards Aerobic Glycolysis During Reperfusion After OGD

Since we found Cdh1 was downregulated after OGD/R, we proposed its ubiquitinated target PFKFB3, also served

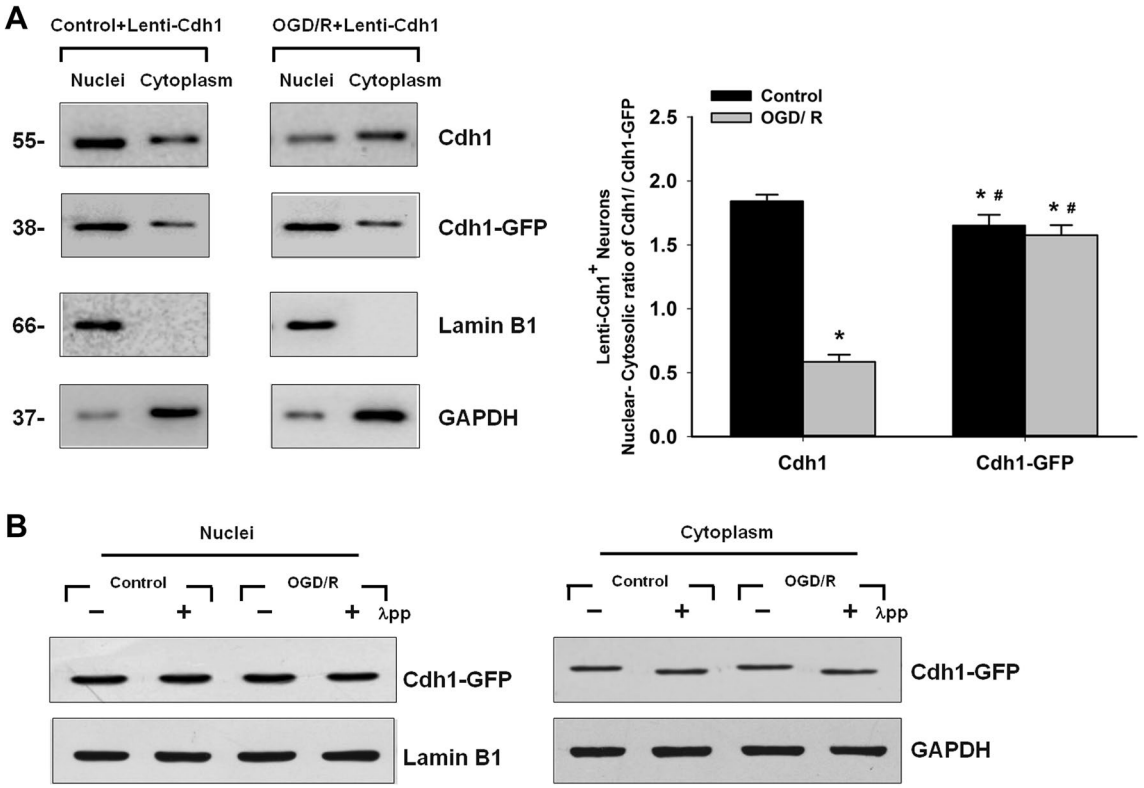

Fig. 3 Localization and phosphorylation status of Cdh1/Cdh1-GFP in control and OGD/R condition. The neurons were infected with Lenti-Cdh1 and then were exposed to control or OGD/R, followed by cell fraction. **a** OGD/R-induced endogenous Cdh1 transport from nuclei to cytoplasm. However, the fusion protein of Cdh1-GFP localized predominantly to nuclear fraction with a few amount distributed in the cytoplasm in the control group. OGD/R did not alter the localization of Cdh1-GFP, which remained mainly at the nuclei. Meanwhile, the cytoplasmic Cdh1-GFP migration in SDS–PAGE was slowed-shifted than nuclear Cdh1-GFP, suggesting a post-translational modification on Cdh1-GFP protein in cytoplasm, such as phosphorylation. Lamin B1 and GAPDH were used as loading controls for nuclei and cytoplasm, respectively. Bar graph represents the nuclear-cytoplasmic ratio of Cdh1 and Cdh1-GFP band intensity (right panel). Data from three independent experiments are shown as mean ± SD. $^{*}P<0.05$, $^{\#}P<0.05$ vs the nuclear-cytoplasmic ratio of endogenous Cdh1 in Control and OGD/R group. **b** The nuclear and cytoplasmic protein extracts were treated with protein phosphatase (λpp). λpp treatment converted the cytoplasmic Cdh1-GFP shifted band to the fast-migrating form, while it had no effect on the migration speed of the nuclear band, in both control and OGD/ R group, suggesting that the predominantly nuclei-localized Cdh1-GFP were non-phosphorylated, whereas the sparsely cytoplasm-distributed Cdh1-GFP were phosphorylated

as the glycolytic key enzyme, may be activated and then affect neuronal metabolism during the reperfusion period. As shown in Fig. 4a, PFKFB3 protein was undetectable in normoxic neurons, but it was highly expressed in the reperfusion state following 1-h OGD, however, this elevation could be efficiently suppressed by Cdh1 lentivirus pretreatment, indicating that OGD-induced Cdh1 reduction was responsible for PFKFB3 accumulation. Meanwhile, a slump of G6PD was also observed during reperfusion after OGD, which could also be reversed by Cdh1 overexpressing (Fig. 4b). To further elucidate whether Cdh1 deficiency-dependent upregulation of PFKFB3 in neurons under OGD/R condition could consequently influence glucose oxidation, we performed radioisotope tracing to evaluate glycolysis and PPP rate. We found that normoxic neurons had relatively low glycolysis and high PPP rate, due to the PFKFB3 absence and G6PD abundance. However, the neurons preferred glycolysis at 12 h of reperfusion when glucose and oxygen delivery has been reestablished, and meanwhile, the branch of PPP was reduced. This change could be inhibited by pretreatment of Cdh1 expressing lentivirus. Moreover, the effect of Cdh1 overexpressing on neuronal glucose utilization under OGD/R could be abolished when co-transfecting with Ken box-mut-PFKFB3 (Cdh1 insensitive PFKFB3 mutant) (Fig. 4c, d). These results demonstrated that Cdh1-mediated PFKFB3 activity was responsible for determining neuronal glucose metabolic pathway during reperfusion after OGD. In addition, the low glycolytic and high PPP state restored by Lenti-Cdh1 under OGD/R condition could be eliminated by overexpression of PFK-1, suggesting an inverse relationship between the activities of glycolysis and PPP during reperfusion of OGD neurons.

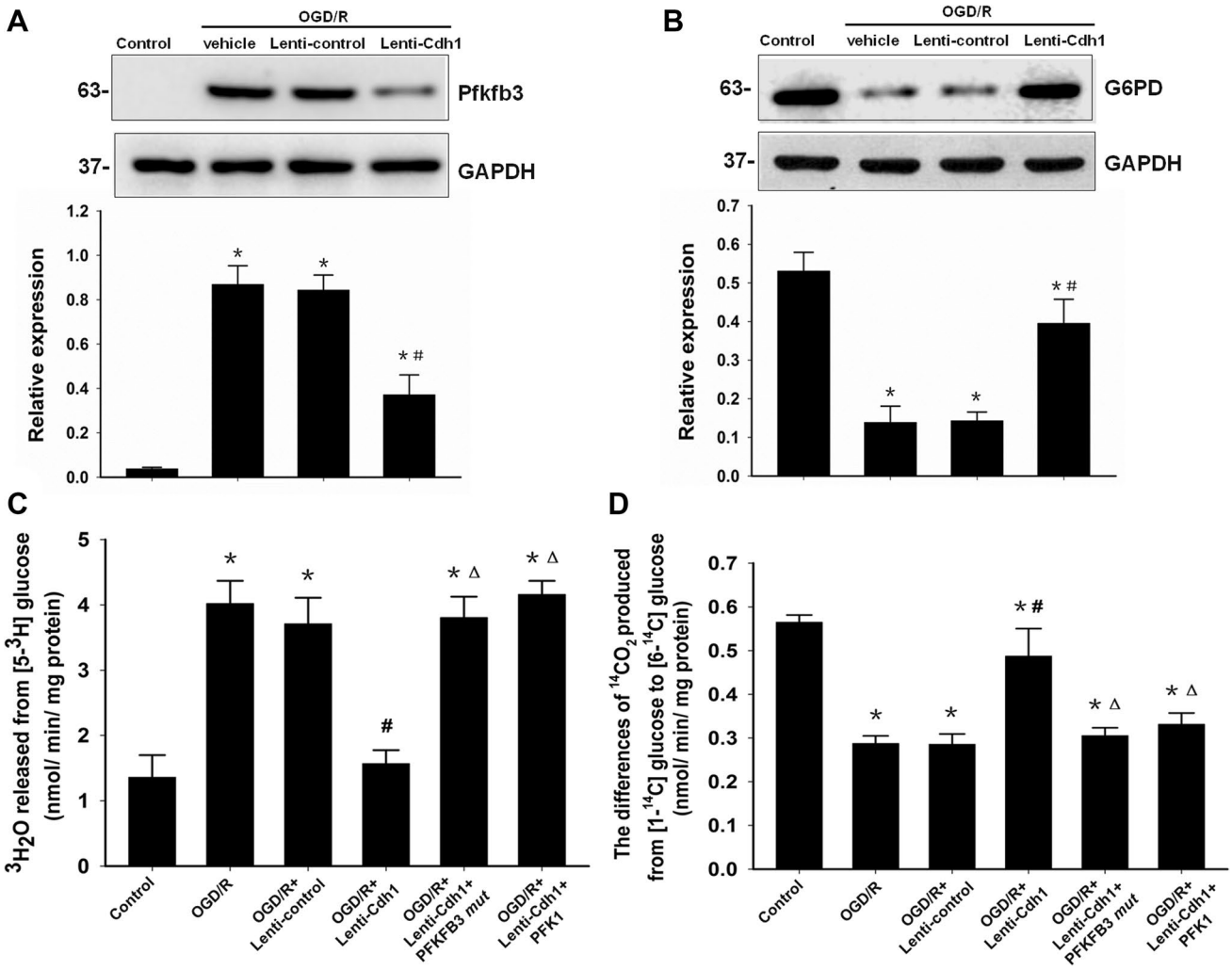

Fig. 4 OGD/R increased neuronal glucose metabolism through glycolysis and decreased PPP activity, which could be inhibited by Cdh1 overexpression. In control neurons, the protein expression of the glycolytic key enzyme PFKFB3 was absent (**a**), whereas the G6PD, PPP key enzyme, was highly expressed (**b**), measured by Western Blot using specific antibodies, which contributed to keep neurons in low glycolytic and high PPP state, measured as the rate of ^3H_2O production from [5-^{3}H] glucose and the differences of $^{14}CO_2$ production from [1-^{14}C]-glucose to [6-^{14}C]-glucose, respectively (**c, d**). Compared to the control neurons, PKFPB3 was accumulated (**a**) and G6PD was significantly down-regulated (**b**) following 1-h OGD and 12-h reperfusion, resulting in increased rate of glycolysis and decreased PPP activity (**c, d**). Administration of Cdh1 expressing lentivirus before OGD could inhibit PFKFB3 accumulation and restored glycolysis to the low basal rate during reperfusion (**a, b, c, d**), this effect was abolished by Ken box-mut-PFKFB3 or PFK-1 overexpression (**c, d**). The relative expressions of PFKFB3 and G6PD were quantified by QUANTITY ONE (Bio-Rad) and then normalized to their internal controls (GAPDH). Data from four independent experiments are shown as mean ± SD. $^*P<0.05$ vs Control, $^{\#}P<0.05$ vs OGD/R + Lenti-control, $^{\Delta}P<0.05$ vs OGD/R + Lenti-Cdh1

Pretreatment with Cdh1 Lentivirus Protected Neurons Against OGD/R-Induced Oxidative Stress and Apoptosis Through Regulation of PFKFB3 and Associated Glucose Metabolism

It was known that NADPH can be regenerated by PPP to produce GSH and exert antioxidative effect. We therefore decided to investigate if the glycolysis/PPP switch initiated by Cdh1 deficiency under OGD/R condition contributed to oxidative stress. Intracellular ROS production was assessed by DCF staining and quantified according to optical densities (ODs). Neuronal apoptosis was measured by TUNEL staining, which was triple-labeled with MAP2 and DAPI (Fig. 5a). As expected, TUNEL-positive cells were rarely detected in normoxic neurons (Fig. 5a, b) with relative few ROS production (Fig. 5c) and low cleaved-caspase 3 expression (Fig. 5d), whereas ROS production and cleaved-caspase3 were significantly increased in neurons after exposure to 1-h OGD and 12-h reperfusion. This neuronal damage was attenuated by infecting with Cdh1

lentivirus prior to OGD, resulting in less ROS production, less cleaved caspase3 expression, and an increased number of viable neurons. MAP2 staining also indicated that Cdh1 overexpression reduced cell body swelling and maintained fine neuronal processes (Fig. 5a). Furthermore, besides the total cells, the apoptotic rates of the lentivirus successfully infected neurons were markedly decreased from 70.2 to 57.5% when pretreated with Cdh1 expressing lentivirus then control lentivirus (Supplementary Fig. 3). In addition, the neuroprotection to oxidative damage by Cdh1 lentivirus pretreatment could be blocked when co-transfecting with Ken box-mut-PFKFB3 (Fig. 5c). PFK-1 overexpression could also convert the increase in the proportion of viable neurons under OGD/R condition induced by Cdh1 overexpression (Fig. 5a, b). These results provided the evidence that enhanced glycolysis was responsible for neuronal apoptosis following OGD/R, and Cdh1 played key role in controlling metabolic balance and ROS damage via PFKFB3 pathway.

Discussion

The major findings of this study are (1) that Cdh1 was inactivated in neurons subjected to 1-h OGD and 12-h reperfusion, (2) that the OGD/R-induced Cdh1 inhibition led to PFKFB3 accumulation and G6PD down-regulation, (3) that change of the glucose metabolic key enzymes made neurons exhibited aerobic glycolysis and concomitant low PPP rate in the reperfusion course, which increased neuronal cellular ROS production and apoptosis, (4) that the rescued Cdh1 expression by lentivirus promoted neuronal survival after OGD/R by the mechanism that restored neurons in natural low glycolytic and high PPP state.

APC is a multi-subunit E3 ubiquitin ligase complex playing essential role in cell cycle progress (García-Higuera et al. 2008). APC activity was controlled by its two subunits, Cdc20 and Cdh1, which binds and activates this complex at a different time. APC-Cdc20 complex targets mitotic cyclins and securin for degradation, thus triggering metaphase–anaphase transition, whereas, in late mitosis, Cdc20 was ubiquitylated and replaced by Cdh1 to form the APC-Cdh1 complex that targets multiple cell cycle regulators for maintaining cells in G1 phase and preventing unscheduled S phase entry (Eguren et al. 2011; Peters 2006). Besides its effects on proliferating cells, APC-Cdh1 was also discovered to be highly expressed in terminally differentiated neurons with critical roles in control of axonal growth, synaptic development, neuronal differentiation, and neuronal excitotoxicity (Gieffer et al. 1999; Kannan et al. 2012; Fu et al. 2011; Yao et al. 2010; Rodriguez-Rodriguez et al. 2012; Vincent et al. 1997). Recently, APC-Cdh1 signaling has been shown to link glucose metabolism and antioxidant defense in neurons at the normal state, however, its involvement in the oxidative damage following ischemia and reperfusion insult remains unknown. Our previous study reported that Cdh1 exported to cytoplasm from nuclei of rat brain neurons after global cerebral ischemia and reperfusion. This phenomenon was also observed following in vitro model of OGD/R in our present study. This result, together with previous reports that nuclear export of Cdh1 was phosphorylation-dependent that leads to inactivation of APC-Cdh1(Jaquenoud et al. 2002; Zhou et al. 2003) and the observed accumulation of downstream substrates Skp2 and SnoN, indicated Cdh1 was inactivated after ischemia/reperfusion damage.

A continuous supply of oxygen and glucose to brain is essential for mitochondrial metabolism to generate energy in the form of adenosine triphosphate (ATP) through the oxidative phosphorylation (OXPHOS). OGD restricts glucose and oxygen supply leading to metabolic stress and potential apoptosis. During the early reperfusion phase, an excessive production of ROS from the initiation of OXPHOS upon reoxygenation leads to further oxidative stress to the mitochondria. Subsequently, the injured mitochondria produce more ROS that alter both membrane and pump functions, and contribute to delayed cell death. As seen in this study, the energy depletion caused by mitochondrial depression was compensated for during the late reperfusion phase with enhanced glycolysis. This is of great interest that the neurons preferred glycolysis at 12 h of reperfusion when glucose and oxygen delivery has been reestablished, such a shift in glucose metabolism had originally been discovered in cancer cells and is known as aerobic glycolysis (Warburg effect). Aerobic glycolysis has also been observed in resting and activated brain in recent years, but its effects remain controversial when it occurs in neurons (Raichle and Mintun 2006; Dienel and Cruz 2016; Magistretti 2016). Bas-Orth et al. have shown that increased synaptic activity could mediate Warburg effect in neurons that may promote mitochondrial homeostasis and neuroprotection (Bas-Orth et al. 2017). Newington et al. have shown that Warburg effect mediated amyloid beta (Aβ) resistance in nerve cell lines that might account for the apoptotic-resistance mechanisms in the surviving neurons of Alzheimer's disease (Newington et al. 2011). Here, we found that in contrast to the absence in normoxic control, PFKFB3 was highly expressed with increased glycolytic rate in primary neurons at 12 h of reperfusion after OGD. This, however, was accompanied by a marked decrease of G6PD and PPP rate resulting in elevated ROS content and apoptosis.

In the brain, PFKFB3 is the most abundant PFKFB isoforms which is distinguished by its very high phosphatase activity to generate fructose-2,6-bisphosphate ($F2,6P_2$) (Ventura et al. 1991). Glycolysis is controlled by its rate-limiting enzyme, 6-phosphofructo- 1-kinase (PFK1), the activity of which is highly dependent on its positive activator $F2,6P_2$. Thereby, the abundance of PFKFB3 protein,

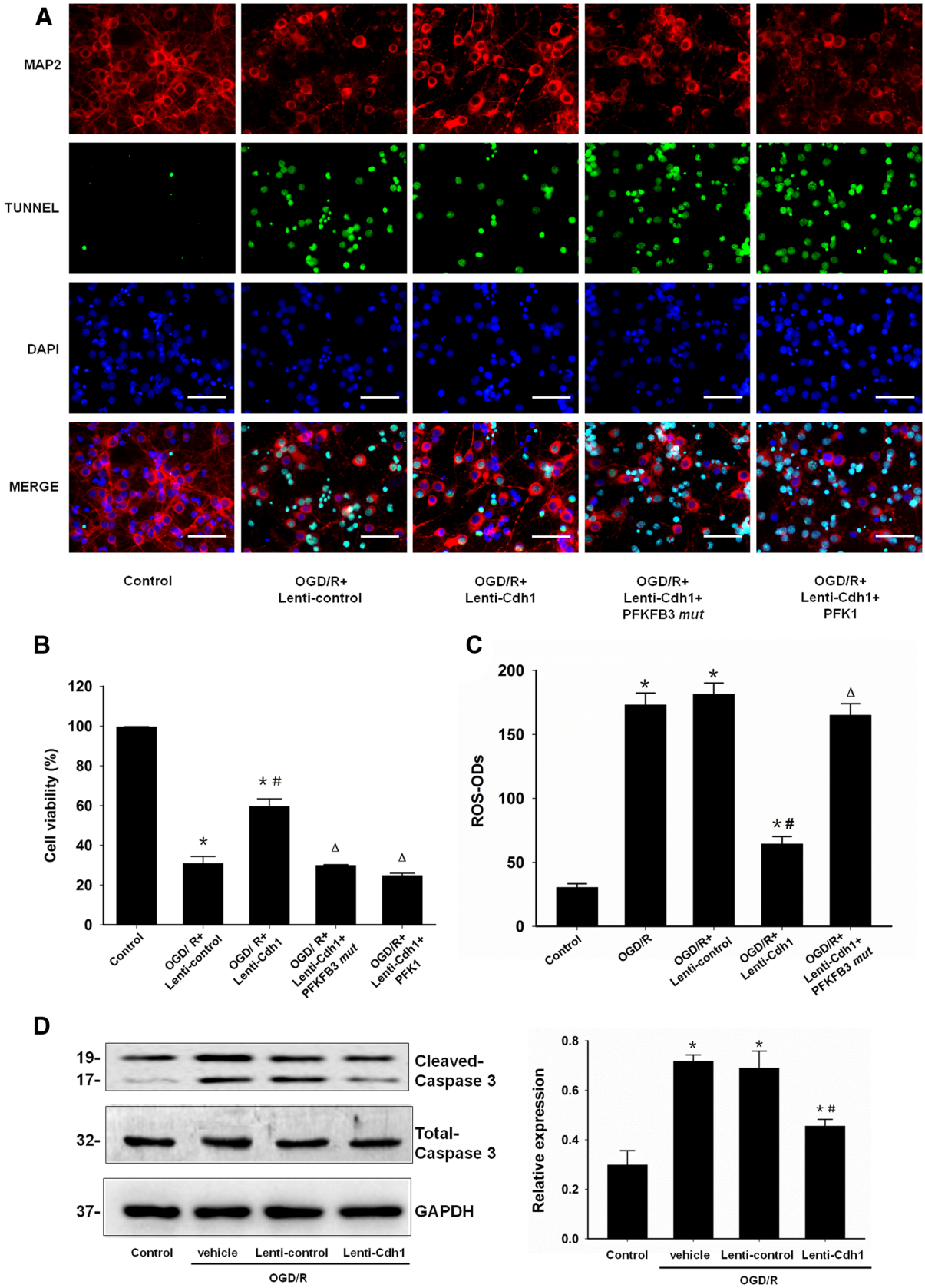
A
MAP2
TUNNEL
DAPI
MERGE
Control
OGD/R+ Lenti-control
OGD/R+ Lenti-Cdh1
OGD/R+ Lenti-Cdh1+ PFKFB3 mut
OGD/R+ Lenti-Cdh1+ PFK1
B
Cell viability (%)
120
100
80
60
40
20
0
Control
OGD/ R+ Lenti-control
OGD/ R+ Lenti-Cdh1
OGD/ R+ Lenti-Cdh1+ PFKFB3 mut
OGD/R+ Lenti-Cdh1+ PFK1
C
ROS-ODs
200
150
100
50
0
Control
OGD/R
OGD/R+ Lenti-control
OGD/R+ Lenti-Cdh1
OGD/R+ Lenti-Cdh1+ PFKFB3 mut
D
19-
17-
Cleaved-Caspase 3
32-
Total-Caspase 3
37-
GAPDH
Control
vehicle
Lenti-control
Lenti-Cdh1
OGD/R
Relative expression
0.8
0.6
0.4
0.2
0.0
Control
vehicle
Lenti-control
Lenti-Cdh1
OGD/R

◂**Fig. 5** Cdh1 protected neurons against OGD/R-induced oxidative stress and apoptosis through regulation of PFKFB3 and associated glucose metabolism. Neurons were infected with control lentivirus or Cdh1 expressing lentivirus alone or in combination with Ken box-mut-PFKFB3 or PFK-1 plasmid vector. 72 h after infection, cells were exposed to 1-h OGD and 12-h reperfusion. **a, b** Compared with control, apoptotic neuronal death was significantly increased in OGD/R + Lenti-control group, as measured by TUNEL staining. This effect was prevented by infecting Cdh1 expressing lentivirus. Meanwhile, infecting neurons with Cdh1 expression lentivirus plus Ken box-mut-PFKFB3 or PFK-1 plasmid prior to OGD markedly eliminated Cdh1 overexpression-mediated pro-survival effect, which increased TUNEL-positive cells to similar levels of OGD/R group. **a** Neurons were labeled with MAP2 (red), TUNEL (green), and DAPI (blue). The vital neurons percentage was calculated by counting TUNEL-negative cells to DAPI staining cells. Three different fields of view on each coverslip were counted from three independent trials. Scale bars, 50 μm. **b** Bar graph represents percentage of vital neurons with value shown as Mean ± SD. **c** OGD/R increased ROS in neurons, as measured by DCFHDA staining by Microplate Reader. Compared with OGD/R + Lenti-control group, infecting Cdh1 expressing lentivirus significantly reduced ROS production following OGD/R damage, this antioxidative effect by Cdh1 overexpression was eliminated when co-transfected with Ken box-mut-PFKFB3. **d** Western Blot revealed the increase of cleaved-caspase 3 in OGD/R neurons. Compared with OGD/R and OGD/R + Lenti-control group, cleaved-caspase 3 was significantly decreased in OGD/R + Lenti-Cdh1 group. $^{*}P < 0.05$ vs Control; $^{\#}P < 0.05$ vs OGD/R + Lenti-control group, $^{\Delta}P < 0.05$ vs OGD/R + Lenti-Cdh1

serves as a reflection of F2,6P_2 levels, can dictate the glycolytic flux. Recent studies revealed that PFKFB3 contains a KEN box at position 142 as a ubiquitylation target by the APC-Cdh1(Herrero-Mendez et al. 2009). To test if decrease of APC-Cdh1 triggered by OGD was responsible for the observed aerobic glycolysis in neurons during reperfusion, we pretreated neurons with Cdh1 expressing lentivirus before OGD. The localization and phosphorylation status of Cdh1-GFP expressed in neurons after infection were also confirmed. In contrast to endogenous Cdh1, Cdh1-GFP was steadily predominantly nuclear and non-phosphorylated, which remained active and exerted ubiquitinated degradation function to substrates in both control and OGD/R group. Furthermore, we found that Cdh1 overexpressing inhibited PFKFB3 protein accumulation and made glucose consumption through glycolysis decreased back to the basal rate under normoxic condition, this effect was abolished by co-infecting with Ken box-mut-PFKFB3. Thus, the enhanced glycolysis in reperfused neurons can be accounted for by Cdh1 deficiency-mediated PFKFB3 accumulation.

Since PPP and glycolysis are metabolically linked for sharing the common intermediate G6P, the increased neuronal glycolysis during reperfusion concomitantly led to decreased PPP rate. Moreover, G6PD, the rate-limiting enzyme of PPP, was found to be decreased during reperfusion in this study. Previous reports demonstrated that cellular stress would cause Tp53-induced glycolysis and apoptosis regulator (TIGAR) activation (Madan et al. 2012). Interestingly, it should be noted that differential expression dynamics of P53, which depends on cell types and stress extent, may lead to different downstream responds to TIGAR activation. It was reported that TIGAR activation lowered F2,6P_2, increased G6PD levels in cancer cells such as U20S and A2780 under mild stress, and thereby block glycolysis and promote PPP activity (Bensaad et al. 2006; Cheung et al. 2012). However, TIGAR activation in renal outermedullary proximal straight tubules (PSTs) resulted in reduced G6PD activity and NADPH levels during reperfusion after severe renal ischemia, contrary to that, G6PD activity and NADPH levels were restored under mild ischemia and reperfusion (Kim et al. 2015). Here, our data showed that G6PD was markedly reduced in primary cortical neurons after relative medium damage of 1-h OGD and 12 reperfusion, and this effect could be abolished by Cdh1 overexpression. Meanwhile, previous study has also shown that genetic ablation of Cdh1 impaired the ability of APC to promote neurogenesis, which caused replicative stress and P53-mediated apoptosis, resulting in decreased number of cortical neurons and cortex size (Delgado-Esteban et al. 2013). Thus, Cdh1 decrease, via P53-mediated TIGAR pathway, might be responsible for G6PD suppression after OGD/ reperfusion insult, but the detailed mechanism remains to be further clarified.

The aerobic glycolysis was believed to provide advantage for cancer cell survival, however, it has rarely been examined in neurons. The neurons naturally express low glycolysis rate due to the absence of PFKFB3. In this study, we found a shift of neuronal glucose metabolism from PPP towards aerobic glycolysis following OGD/R damage. Although many researches over the last decades have shown that the so-called Warburg effect provides beneficial effects of reduced mitochondrial respiration and associated ROS production that trigger apoptosis (Bonnet et al. 2007; Sun et al. 2016), it may have detrimental effects when it occurs in neurons, as enhanced glycolysis diverts glucose metabolism away from PPP, resulting in decreased antioxidant levels of NADPH and GSH. Our data demonstrated that the metabolic shift initiated by Cdh1 depletion following OGD/R was accompanied by oxidative stress, as revealed by increased ROS production, cleaved-caspase 3, as well as neuronal apoptosis. This result indicated that PPP always has priority to maintain neuronal antioxidant status, the inhibition of which following enhanced glycolysis would dampen the protective mitochondrial suppression elicited by Warburg effect under OGD/R condition. Indeed, we showed that overexpressing Cdh1 in neurons by lentivirus prior to OGD, which effectively reduced PFKFB3 and increased G6PD expression, prevented the glycolysis/PPP shift and subsequently maintained neuronal redox homeostasis by scavenging ROS during reperfusion stage.

Conclusion

Collectively, we have shown for the first time that a Warburg effect exists in neurons subjected to OGD/R injury, which is attributed to APC-Cdh1 deficiency and concomitant PFKFB3 accumulation. This metabolic shift impairs the NADPH-GSH recycling, resulting in an increased sensitivity of neurons to oxidative damage. Administration of Cdh1 expressing lentivirus efficiently enhanced neuronal viability under oxidative stress via maintaining neurons in the natural low glycolysis and high PPP state. Thus, our observation suggests that apart from the anti-aberrant cell cycle entry role of APC-Cdh1 in neurons, it is also an important target for antioxidative apoptosis following OGD/R through mechanisms that modulate metabolic pathways.

Acknowledgements This work was supported by the National Natural Science Foundation of China (Grant No. 81600965).

Author Contributions YZ and LW designed the study; ZL and BZ performed the experiments; ZL and WY collected the data and performed the analysis; ZL and CZ wrote the initial draft; YZ contributed towards manuscript improvement and revision.

Compliance with Ethical Standards

Conflict of interest The author(s) declared they have no financial relationship with the organization that sponsored the research and have no potential conflicts of interest with respect to the research, authorship, and/or publication of this article.

References

Bashir T, Dorrello N, Amador V, Guardavaccaro D, Pagano M (2004) Control of the SCF (Skp2-Cks1) ubiquitin ligase by the APC/C (Cdh1) ubiquitin ligase. Nature 428:190–193

Bas-Orth C, Tan YW, Lau D, Bading H (2017) Synaptic activity drives genomic program that promots a neuronal Warburg effect. J Biol Chem 292(13):5183–5194

Bensaad K, Tsuruta A, Selak MA, Vidal MN, Nakano K, Bartron R, Gottlieb E, Vousden K. H (2006) TIGAR, a p53-inducible regulator of glycolysis and apoptosis. Cell 126:107–120

Bolaños JP, Almeida A (2010) The Pentose-Phosphate Pathway in Neuronal Survival Against Nitrosative Stress. IUBMB Life 62:14–18

Bolaños JP, Delgado-Esteban M, Herrero-Mendez A, Fernandez-Fernandez S, Almeida A (2008) Regulation of glycolysis and pentose–phosphate pathway by nitric oxide: Impact on neuronal survival. Trends Biochem Sci 35:145–149

Bolaños JP, Almeida A, Moncada S (2010) Glycolysis: a bioenergetic or a survival pathway? Trends Biochem Sci 35:145–149

Bonnet S, Archer SL, Allalunis-Turner J, Haromy A, Beaulieu C, Thompson R, Lee CT, Lopaschuk GD, Puttagunta L, Bonnet S, Harry G, Hashimoto K, Porter CJ, Andrade MA, Thebaud B, Michelakis ED (2007) A mitochondria-K^+ channel axis is suppressed in cancer and its normalization promotes apoptosis and inhibits cancer growth. Cancer Cell 11:37–51

Chan PH (2001) Reactive oxygen radicals in signaling and damage in the ischemic brain. J Cereb Blood Flow Metab 21:2–14

Cheung EC, Ludwig RL, Vousden KH (2012) Mitochondrial localization of TIGAR under hypoxia stimulates HK2 and lowers ROS and cell death. Proc Natl Acad Sci USA 109:20491–20496

Delgado-Esteban M, Garcia-Higuera I, Maestre C, Moreno S, Almeida A (2013) APC/C-Cdh1 coordinates neurogenesis and cortical size during development. Nat Commun 4:2879

Dienel GA, Cruz NF (2016) Aerobic glycolysis during brain activation: adrenergic regulation and influence of norepinephrine on astrocytic metabolism. J Neurochem 138:14–52

Eguren M, Manchado E, Malumbres M (2011) Non-mitotic functions of the anaphase-promoting complex. Semin Cell Dev Biol 22:572–578

Fu AK, Hung KW, Fu WY, Shen C, Chen Y, Xia J, Lai KO, Lp NY (2011) APC (Cdh1) mediates EphA4-dependent downregulation of AMPA receptors in homeostatic plasticity. Nat Neurosci 14:181–189

García-Higuera I, Manchado E, Dubus P, Cañamero M, Méndez J, Moreno S, Malumbres M (2008) Genomic stability and tumour suppression by the APC/C cofactor Cdh1. Nat cell boil 10:802–811

Garcia-Nogales P, Almeida A, Bolaños JP (2003) Peroxynitrite protects neurons against nitric oxide-mediated apoptosis. A key role for glucose-6-phosphate dehydrogenase activity in neuroprotection. J Biol Chem 278:864–874

Gieffers C, Peters BH, Kramer ER, Dotti CG, Peters JM (1999) Expression of the CDH1-associated form of the anaphase-promoting complex in postmitotic neurons. Proc Natl Acad Sci USA 96:11317–11322

Herrero-Mendez A, Almeida A, Fernandez E, Maestre C, Moncada S, Bolaños JP (2009) The bioenergetic and antioxidant status of neurons is controlled by continuous degradation of a key glycolytic enzyme by APC/C-Cdh1. Nat Cell Biol 11:747–752

Hu R, Li L, Li D, Tan W, Wan L, Zhu C, Zhang Y, Zhang C, Yao W (2016) Downregulation of Cdh1 signaling in spinal dorsal horn contributes to the maintenance of mechanical allodynia after nerve injury in rats. Mol Pain 12:1–16

Huang XJ, Zhang WP, Li CT, Shi WZ, Fang SH, Lu YB, Chen Z, Wei EQ (2008) Activation of CysLT receptors induces astrocyte proliferation and death after oxygen–glucose deprivation. Glia 56:27–37

Jaquenoud M, van Drogen F, Peter M (2002) Cell cycle-dependent nuclear export of Cdh1p may contribute to the inactivation of APC/C(Cdh1). EMBO J 21:6515–6526

Kannan M, Lee SJ, Schwedhelm-Domeyer N, Stegmüller J (2012) The E3 ligase Cdh1-anaphase promoting complex operates upstream of the E3 ligase Smurf1 in the control of axon growth. Development 139:3600–3612

Kim J, Devalaraja-Narashimha K, Padanilam BJ (2015) TIGAR regulates glycolysis in ischemic kidney proximal tubules. Am J Physiol Renal Physiol 308:F298–F308

Larrabee MG (1990) Evaluation of the pentose phosphate pathway from $^{14}CO_2$ data. Fallibility of a classic equation when applied to non-homogeneous tissues. Biochem J 272:127–132

Liu PK, Grossman RG, Hsu CY, Robertson CS (2001) Ischemic injury and faulty gene transcripts in the brain. Trends Neurosci 24:581–588

Lv Y, Zhang B, Zhai C, Zhang Y, Yao W, Zhang C (2015) PFKFB3-mediated glycolysis is involved in reactive astrocyte proliferation after oxygen-glucose deprivation/ reperfusion and is regulated by Cdh1. Neurochem Int 91:26–33

Madan E, Gogna R, Kuppusamy P, Bhatt M, Pati U, Mahdi AA (2012) TIGAR induces p53-mediated cell-cycle arrest by regulation of RB-E2F1 complex. Br J Cancer 107:516–526

Magistretti PJ (2016) Imaging brain aerobic glycolysis as a marker of synaptic plasticity. Proc Natl Acad Sci USA 113: 7015–7016

McLaughlin BA, Nelson D, Silver IA, Erecinska M, Chesselet MF (1998) Methylmalonate toxicity in primary neuronal cultures. Neuroscience 86:279–290

Newington JT, Pitts A, Chien A, Arseneault R, Schubert D, Cumming RC (2011) Amyloid beta resistance in nerve cell lines is mediated by the Warburg effect. PLoS ONE 6(4):e19191

Peters JM (2006) The anaphase promoting complex/cyclosome: a machine designed to destroy. Nat Rev Mol Cell Biol 7:644–656

Qiu J, Zhang C, Lv Y, Zhang Y, Zhu C, Wang X, Yao W (2013) Cdh1 inhibits reactive astrocyte proliferation after oxygen-glucose deprivation and reperfusion. Neurochem Int 63:87–92

Raichle ME, Mintun MA (2006) Brain work and brain imaging. Annu Rev Neurosci 29:449–476

Rodriguez-Rodriguez P, Fernandez E, Almeida A, Bolaños JP (2012) Excitotoxic stimulus stabilizes PFKFB3 causing pentose-phosphate pathway to glycolysis switch and neurodegeneration. Cell Death Differ 19:1582–1589

Schapira AH (2009) Neurobiology and treatment of Parkinson's disease. Trends Pharmacol Sci 30:41–47

Stegmüller J, Konishi Y, Huynh M, Yuan Z, Dibacco S, Bonni A (2006) Cell-intrinsic regulation of axonal morphogenesis by the Cdh1-APC target SnoN. Neuron 50:389–400

Støttrup NB, Løfgren B, Birkler RD, Nielsen JM, Wang L, Caldarone CA, Kristiansen SB, Contractor H, Johannsen M, Bøtker HE, Nielsen TT (2010) Inhibition of the malate–aspartate shuttle by pre-ischaemic aminooxyacetate loading of the heart induces cardioprotection. Cardiovasc Res 88:257–266

Sun JH, Ren XF, Qi W, Yuan D, Simpkin JW (2016) Geissoschizine Methyl ether protects oxidative stress-mediated cytotoxicity in neurons through the 'Neuronal Warburg Effect'. J Ethnopharmacol 187:249–258

Tan W, Yao W, Hu R, Lv Y, Wan L, Zhang C, Zhu C (2015) Alleviating neuropathic pain mechanical allodynia by increasing Cdh1 in the anterior cingulate cortex. Mol Pain 11:56

TeSlaa T, Teitell MA (2014) Techniques to monitor glycolysis. Methods Enzymol 542:91–114

Vander Heiden MG, Christofk HR, Schuman E, Subtelny AO, Sharfi H, Harlow EE, Xian J, Cantlay LC (2010) Identification of small molecule inhibitors of pyruvate kinase M2. Pharm Biol 79:1118–1124

Ventura F, Rosa JL, Ambrosio S, Gil J, Bartrons R (1991) 6-phosphofructo-2-kinase/fructose-2,6-bisphosphatase in rat brain. Biochem J 276:455–460

Vincent I, Jicha G, Rosado M, Dickson D (1997) Aberrant expression of mitotic cdc2/cyclin B1 kinase in degenerating neurons of Alzheimer's disease brain. J Neurosci 17:3588–3598

Yao W, Qian W, Zhu C, Gui L, Qiu J, Zhang C (2010) Cdh1-APC is involved in the differentiation of neural stem cells into neurons. Neuroreport 21:39–44

Zhang Y, Yao W, Qiu J, Qian W, Zhu C, Zhang C (2011) The involvement of down-regulation of Cdh1–APC in hippocampal neuronal apoptosis after global cerebral ischemia in rat. Neurosci Lett 505:71–75

Zhang B, Wei K, Li X, Hu R, Qiu J, Zhang Y, Yao W, Zhang C, Zhu C (2018) Upregulation of Cdh1 signaling in the hippocampus attenuates brain damage after transient global cerebral ischemia in rats. Neurochem Int 112:166–178

Zhou Y, Ching YP, Chun AC, Jin DY (2003) Nuclear localization of the cell cycle regulator CDH1 and its regulation by phosphoryla- tion. J Biol Chem 278:12530–12536